NAP-2013

Morphology of Silver Nanoparticles in the Graft Copolymer Matrices

S.V. Fedorchuk[1,*], T.B. Zheltonozhskaya[1,†], Yu.P. Gomza[2,°], S.D. Nessin[2,°], D.O. Klymchuk[3,+]

[1] *Kiev National University of Taras Shevchenko, Faculty of Chemistry, Department of Macromolecular Chemistry,*
60 Vladimirskaya St, 01033 Kiev, Ukraine
[2] *Institute for Macromolecular Chemistry, National Academy of Sciences of Ukraine,*
48 Kharkovskoye Shosse, 02160 Kiev, Ukraine
[3] *Institute of Botany, National Academy of Sciences of Ukraine, 2 Tereschenkovskaya St., 01601 Kiev, Ukraine*

In the present work, we used two-component graft copolymers PVA-*g*-PAAm based on poly(vinyl alcohol) and chemically complementary polyacrylamide as special templates in the process of borohidride reduction of Ag+ ions. It was established the influence of molecular architecture and concentration of the matrices and the content of silver nitrate on some reaction parameters, size, stability and morphology of Ag-nanoparticles in aqueous solutions.

Keywords: Nanoparticles, Matrix, Self-assembly, Supramolecular structures, X-ray scattering.

PACS numbers: 82.35.Jk, 61.46.Df

1. INTRODUCTION

Metallic nanoparticles have fascinated scientists because of their colorful colloidal solutions long before semiconductors and their applications became an integral part of modern technology. Although the synthesis and the physical characterization of metal nanocrystals have been generally investigated, considerably less attention has been devoted to the fabrication of novel nanostructured materials [1-5]. However, the high chemical activity of zero-valent metals can cause the irreversible aggregation of the nanoparticles that creates the problem of their storage stability. In order to solve this problem, the development of the nanoparticle synthesis methods in polymer matrices, which will ensure the control of nanoparticle sizes, forms and stabilization in a solution, is necessary. Last time, the graft copolymers, which form micellar structures, are used to obtain the Ag-containing nanosystems mainly in organic medium [6,7]. However, in separate cases (for example, at the use of silver nanoparticles in medicine and catalysis of chemical reactions) the nanoparticles should be obtained and stabilized in a hydrophilic environment.

In the present work, was investigation products of the Ag+ ions chemical (borohidryde) reduction from silver nitrate in aqueous solutions of the IntraPC-forming graft copolymers with hydrophilic biocompatible and partially biodegradable blocks of a variable length and there morphology.

2. EXPERIMENTAL

2.1 Materials and syntheses

We carried out syntheses of PVA-*g*-PAAm using the template radical graft copolymerization, which was initiated by the Red/Ox reaction of cerium ammonium

nitrate with hydroxyl groups of PVA [8, 9].

The reagents were mixed in the deionized water and inert atmosphere at 25 °C for 24 h. The Ce[IV] complex salt (cerium ammonium nitrate) was used as an oxidant but hydroxyl groups of PVA were as reducing agents [10].

$$\text{C—OH} + \text{Ce}^{\text{IV}} \longrightarrow \text{complex}(\text{C—\"OH}) \longrightarrow \text{C—\.O} + \text{Ce}^{\text{III}} + \text{H}^+$$
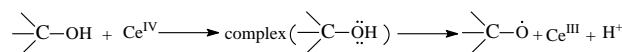
The template character of the graft copolymerization in the cases of chemically complementary PVA and PAAm was proved in the study [9]. Gel-like graft copolymers were diluted by water, re-precipitated by acetone, dissolved again in water and freeze-dried. The samples of PVA with M_v = 90 kDa and cerium ammonium nitrate from "Aldrich" (USA) and acrylamide (AAm) from "Reanal" (Hungary) were used in the syntheses. The following molar ratios of the reagents: [Ce[IV]]/[PVA] = 25 and the monomer concentration equaled to 1 mol·m⁻³ were used in the syntheses. The reagents blends in deionized water were stirred in an inert atmosphere at 20 ÷ 25 °C for 24 h. Characterization of PVA-*g*-PAAm was performed first by an elemental analysis on C, H, N. Further, the dialysis of the reaction blend against deionized water were performed and the molecular weight of PAAm was found by viscometry (M_{vPAAm} = 147 (PVA-*g*-PAAm1) and 65 kDa (PVA-*g*-PAAm2)). The average number of the grafts per PVA-*g*-PAAm macromolecule (PVA-*g*-PAAm1 N = 10 and PVA-*g*-PAAm2 N = 22) was calculated from these data [11]. Macromolecules of PVA-*g*-PAAm with chemically complementary components and a low density of the grafts formed the micelle-like associates [11], which "corona" included the PAAm surplus segments unbonded with PVA.

The reduction of silver ions was carried out in aque-

* sergey_fedorchuk@ukr.net
† zheltonozhskaya@ukr.net
° polymer7@ukr.net
+ microscopy.botany@gmail.com

ous polymer solutions with the eightfold molar excess of NaBH$_4$ that allowed achieving practically complete conversion of Ag$^+$ ions to zero-valent state in a selected region of AgNO$_3$ concentrations (C_{AgNO3} = 0.91 ·10^{-2} and 1.82 ·10^{-2} kg·m^{-3}) [12], according to the studies [13].

At the same time, borohydride anions participate also in some side reactions, due to which their essential excess is used to enhance the yield of Ag nanoparticles [12].

Polymeric solutions was mixed with AgNO$_3$ and kept for 30 min in a dark box; then the reducing agent was added. We varied concentrations of the polymeric matrices (C_m = 0.5, 1.0 and 2.0 kg·m^{-3}) and silver salt (see above)**.**

2.2 Characterization

The process of nanoparticle formation was controlled by the changes in the position (λ_{max}) and the integral intensity (S) of the surface plasmon resonance band (SPRB), which was displayed in a visible region of spectrum [4,6]. The time evolution of the extinction spectra was recorded in a three-minute interval in a region of 200 ÷ 1000 nm using a Cary 50 Scan UV-Vis spectrometer from "Varian" (USA).

WAXS profiles for the dried compositions were obtained in a cell with a thickness of 2 mm using a DRON-2.0 X-ray difractometer with Ni-filter in a primary beam. The monochromatic Cu-K$_\alpha$ radiation with λ = 0.154 nm, filtered by Ni, was provided by an IRIS M7 generator (at operating voltage of 30 kV and a current of 30 mA). The scattered intensities were measured by a scintillation detector scanning in 0.2° steps over the range of the θ = 3-45° scattering angles (corresponding to q = 2.13-31.21 nm^{-1}, where $q = 4\pi sin(\theta/2)/\lambda$ is the wavevector or the scattering vector). The diffraction curves obtained were reduced to equal intensities of the primary beam and equal values of the scattering volume [14]. Also, the normalization of experimental scattered intensities was carried out according to the formula:

$$I_{n(i)}(\theta) = [I_{\exp}(\theta) - I_b(\theta)] \cdot (I/I_0)$$

where $I_{exp}(\theta)$ and $I_{n(i)}(\theta)$ are the experimental and normalized intensities in WAXS profile as a function of θ, $I_b(\theta)$ is the intensity of the background for every θ value, I_0 and I are the intensities of incident and scattered beams at θ = 0° (the coefficient of the beam weakening).

SAXS profiles for the compositions were obtained in an automated Kratky slit-collimated camera. Here copper anode emission monochromated by total internal reflection and nickel filter was used. The intensity curves were recorded in the step-scanning mode of the scintillation detector in a region of the θ = 0.03 ÷ 4.0° scattering angles (the wavevector q = 0.022-2.86 nm^{-1}). Thus, the study of the micro-scale heterogeneous domains with characteristic dimensions (evaluated as 2π/q) from 2 to 280 nm was possible. Normalization of SAXS profiles was carried out using the FFSAXS-3 program [14] and a standard sample from the laboratory of professor Kratky. The scattered intensities were normalized to the sample thickness and the scattered intensity of a standard. Additionally, the raw intensity curves were smoothed, corrected for parasitic scattering

and desmeared.

TEM images of polymer/silver compositions were obtained with an electron microscope JEM-I23O from "JEOL" (Japan) at a voltage of 90 kV. Small drops (~1 ·10^{-4} cm^3) of the compositions were placed on copper grids covered with Formvar film and carbon, and then quickly dried for 0.5 ÷ 1 min at a room temperature.

3. RESULTS AND DISCUSSION

The state of PVA-*g*-PAAm in aqueous solutions was considered in our previous publications It was shown [15] that asymmetric macromolecules graft copolymerrs formed the "hairy-type" micelles in aqueous medium due to interaction of PVA and PAAm blocks followed by segregation (self-assembly) of non-polar bound parts. Relatively small "core" of these micelles contained non-polar bound parts of both the blocks but the developed "corona" comprised the segments of longer PAAm chains, which were unbound with PVA.

3.1 Kinetics and Products of Borohydride Reduction of Silver Ions

In 3-5 minutes after addition of the reducing agent to the mixtures of PVA-*g*-PAAm, with AgNO$_3$, a yellow coloring, which corresponded to the color of the diluted silver nanodispersions in water [12,16], was appeared. The coloring intensity increased for 1-3 h at C_{AgNO3} = 1.82 ·10^{-2} kg·m^{-3}. But at lower concentrations of silver ions (C_{AgNO3} = 0.91 ·10^{-2} kg·m^{-3}) and at C_m = 0.5 and 1.0 kg·m^{-3}, a yellow color was quickly disappeared and a black precipitate arose. The same picture was observed in the case of Ag$^+$-ion reduction in polymer-free solutions with low concentration of AgNO$_3$. The results for 90 min, which were obtained at the maximum concentrations of the matrices and AgNO$_3$, are shown in Fig 1.

The formation of spherical Ag nanoparticles much smaller than the wavelength of light results in the appearance of a single narrow SPRB with λ_{max} = 380 ÷ 425 nm in the extinction spectra [16, 17]. Exactly such Ag nanoparticles formed in the studied reaction blends that was confirmed by a unimodal narrow SPRB (λ_{max} = 379 ÷ 400 nm), which was observed in all the spectra.
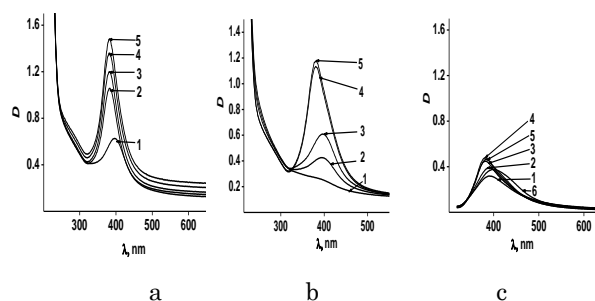

Fig. 1 – The time evolution of the absorption spectra in aqueous blends of (a) PVA-*g*-PAAm1, (b) PVA-*g*-PAAm2 and (c) refers to the same reaction in the polymer-free solution with AgNO$_3$ in 5 -*1*, 15 -*2*, 21 -*3*, 36 -*4*, 60 −*5* and 90 min −*6* after NaBH$_4$ introduction. C_m = 2.0 kg·m^{-3}, C_{AgNO3} = 1.82 ·10^{-2} kg·m^{-3}

At the same time, in polymer-free solutions, such effects as SPRB widening in time and a red shift of λ_{max}

were also revealed (Fig. 1c). In principal, there are some reasons, which could initiate the last effects [17]: i) increase in a size (or polydispersity) of spherical Ag nanoparticles, ii) formation more stretched Ag particles (spheroids, ellipsoids etc.), and iii) aggregation of Ag nanoparticles.

The spectra of all the reaction blends in Fig. 1 demonstrated additionally a weak band in the region of $\lambda = 270 \div 290$ nm. This absorption band is known to reflect the presence of the charged Ag_4^{2+} nanoclusters [17], which arise at the initial stage of silver reduction. PVA-*g*-PAAm1 showed better results, which can be explained by a branched structure, therefore, had been made available for further research.

3.2 Structure of Polymeric Compositions with Silver Nanoparticles

The bulk structure of some polymer-metal compositions was characterized and the size of Ag nanoparticles was determined using wide-angle and small-angle X-ray scattering (WAXS and SAXS). The polymer-metal compositions were cast from aqueous solutions ($C_m = 2.0$ and $C_{AgNO3} = 3.64$ kg·m^{-3}) into special Teflon forms placed in a dark box and then were dried on air and in a vacuum desiccator for 10 days. The results (Fig. 2) showed that the bulk structure of the compositions contained a polymeric amorphous phase, that was displayed in WAXS profiles by two diffusive overlapped maxima at $\theta \sim 15°$ and $21°$, and crystalline Ag nanoparticles, that was confirmed by characteristic crystalline peaks of silver (111) at $\theta \sim 38°$ [18]. The appearance of these peaks indicated the formation of crystalline Ag nanoparticles with tetragonal facet-centered cubic lattice [18]. An amorphous character of polymeric phases in the compositions was completely correlated with the data of DSC studies [15], which demonstrated the loss of PVA crystalline properties in the block copolymer structure because of the interaction of the main and grafted chains.

As to the presence of two diffusive overlapped maxima in WAXS profiles in Fig. 2a, they could be attributed (as in the study [19]) to the presence of two systems of planes of the paracrystalline lattice in the amorphous regions of PVA-*g*-PAAm1 structures, which contain mainly PAAm chains. The first maximum with smaller intensity at $\theta \sim 15.2°$ characterizes the lateral periodicity in an arrangement of PAAm chains but the second one with greater intensity at $\theta \sim 21°$ reflects the periodic arrangement of the flat hydrogen-bonded *cis*-dimers of amide groups in the structures of *cis-trans*-multimers [8].
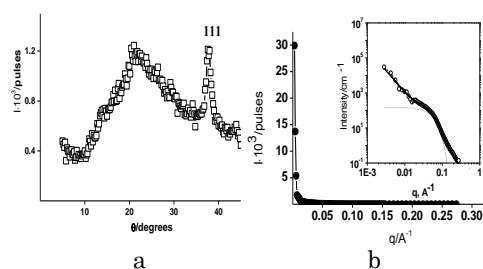

Fig. 2 – WAXS difractogram for the compositions PVA-*g*-PAAm1/Ag (a). The intensity of SAXS *vs* the wavevector for the composition PVA-*g*-PAAm1/Ag (b). The double logarithmic SAXS profiles are shown in a lesser scale. $T = 20$ °C

The results in a form of the dependences of the scattered intensities versus q are shown in Fig. 2b.

All the profiles demonstrated a sharp fall in the scattered intensities with q growth (without any diffraction maxima) that pointed out the absence of any periodicity in the arrangement of structural elements of the compositions and polymer-inorganic hybrid at the supramolecular level. The same profiles in two logarithmic coordinates are exhibited in Fig. 2 b in a lesser scale. Let's carry out their analysis from the point of view the fractal-cluster organization of the composition structure [19].

The double logarithmic SAXS profile for the composition demonstrated two linear parts with different slopes, which corresponded to two power scattering regimes by Porod ($I \approx q^{-Df}$, where D_f is the slope ratio for corresponding straight line of log I *vs* log q). These linear parts were connected by the curve, which conformed to the exponential scattering regime by Guinier [19]. Such form of SAXS profiles in the double logarithmic coordinates pointed out the two-level fractal organization of a bulk structure of the compositions and polymer-inorganic hybrid. The character of separate elements of each level (the mass-fractal clusters, the surface-fractal clusters or solid particles with a smooth surface) could be determined by analysis of D_f value but the maximum diameter of these elements could be estimated by the relation $d_{max} \sim 2\pi/q^*$ [14,19]. Finding the last parameter is possible in the case, when the straight line corresponding to the power scattering regime by Porod is ended (or "cuts") by the scattering regime by Guinier in the region of small q that is when a separate structural level is clearly displayed. A definite q^* value, which is determined in the region of the Guinier's scattering (Fig. 2b) [19], is considered as "the cutting border". All said parameters (D_f, q^* and d_{max}) were established only for the 1-st lower level of structural organization of the compositions, which was displayed at higher q. For the 2-nd higher structural level, which was revealed at less q, only D_f numbers were found (Table 1) because corresponding straight lines of the Porod's scattering in Fig. 2b were not restricted from above by the Guinier's scattering regimes.

It is well known [19], that the $D_f = 4$ value characterizes the power scattering regime by Porod in the case of the dense solid scattering particles with a smooth surface. Exactly such values were determined for the linear parts of SAXS profiles, which corresponded to the 1-st structural level of the compositions (Table 1). This fact additionally confirmed the formation of the dense Ag nanoparticles in both the polymeric matrices. The maximum radius of a gyration for these particles was calculated using d_{max} value and the relation: $[R_g = d_{max}/2(5/3)^{1/2}]$ [19]. Thus, the dense crystalline Ag nanoparticles constituted the 1-st level of the fractal-organized structure of the polymer-metal composites. Using Beaucage's method of global unified exponential-power functions, [15, 19], we modelled SAXS profiles for both compositions taking into consideration two levels of their structural organization, which were discussed above. As a result, the value R_g (calc) for Ag-nanoparticles in the structure of compositions (Table 3) was obtained, which are well consistent with those that were found from the experimental profiles of SAXS,

and was represented virtually the revised values of maximum hydrodynamic radius of the particles.

Table 1 – Parameters of structural elements of the 1-st and 2-nd structural level

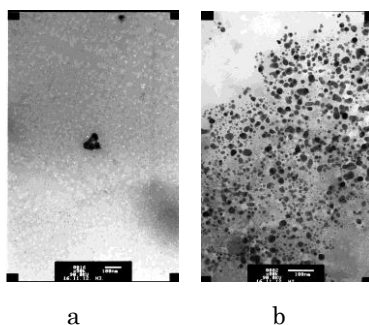| Value \ System	PVA-*g*-PAAm1/Ag	
	1-st	**2-nd**
D_f	4.0	2.6
$q^* \cdot 10^2$ / A^{-1}	6.1	–
d_{max} / nm	10.3	–
R_g / nm	4.0	–
$R_{g\,(calc)}$ / nm	3.5	–

a   b

Fig. 3 – Electron micrograph of micellar structures PVA-*g*-PAAm1/Ag (a) and test system without of polymer (b)

TEM image for the composition clearly demonstrated the presence of two types of Ag-nanoparticles in the polymer matrices (Fig. 3). It was found that the average size of Ag-nanoparticles obtained in PVA-*g*-PAAm1 micellar solution (~4 nm) (Fig. 3a). This fact fully correlated with data of SAXS measurements and calculations represented in Table 1. The formation of essentially larger Ag-nanoparticles (~ 30 nm) was observed in the test system that is in pure water (Fig. 3b). Thus, the high stabilizing activity of the graft copolymers with respect to small Ag-nanoparticles was fully proved.

CONCLUSION

Graft copolymers PVA-*g*-PAAm, which form Intra PCs and self-assemble in micellar structures in aqueous solutions, could be considered as efficient nanoreactors. They are capable of ensuring the high rate and efficacy of the borohydride reduction of silver ions up to the stable crystalline Ag nanoparticles with R_g ~ 4 nm. The composition of PVA-*g*-PAAm1 with Ag nanoparticles showed the two-level fractal organization of their structure. The dense crystalline silver nanoparticles were the separate elements of the 1-st lower level, while the mass-fractal clusters of the polymeric matrices constituted the 2-nd higher structural level. The formation of smaller silver nanoparticles under the influence PVA-*g*-PAAm1 (R_g = 4 nm) was found.

REFERENCES

1. A. Manna, T. Imae, K. Aoi, M. Okada, T. Yogo, *Chem. Mater*. **13**, 1674 (2001).
2. O.M. Wilson, R.W.J. Scott, J.C. Garcia-Martinez, R.M. Crooks, *Chem. Mater*. **16**, 4202 (2004).
3. S. Porel, S. Singh, S.S. Harsha, D.N. Rao, T.P. Radhakrishnan, *Chem. Mater*. **17**, 9 (2005).
4. K. Huber, T. Witte, J. Hollmann, S. Keuker-Baumann, *J. Am. Chem. Soc.* **129**, 1089 (2007).
5. B.H. Sohn, J.M. Choi, S. Yoo, S.H. Yun, W.C. Zin, J.C. Jung, M. Kanehara, T. Hirata, T. Teranishi, *J. Am. Chem. Soc.* **125**, 6368 (2003).
6. W. Schärtl, *Nanoscale* **2,** 829 (2010).
7. S. Horikoshi, H. Abe, K. Torigoe, M. Abe, *Serpone, Nanoscale* **2010**, *2*, 1441.
8. T. Zheltonozhskaya, N. Permyakova, L. Momot, V.V. Khutoryanskiy, G. Staikos, *Hydrogen-Bonded Interpolymer Complexes. Formation, Structure and Applications* Ch.5, (New Jersey-London-Singapore-Beijing etc.: World Scientific 2009).
9. T.B. Zheltonozhskaya, S.V. Fedorchuk, V.G. Syromyatnikov, *Russ. Chem. Rev.* **76**, 731 (2007).
10. D.G. Angelescu, M. Vasilescu, R. Somoghi, D. Donescu, V.S. Teodorescu, *Colloids and Surfaces A: Physicochem Eng. Asp.* **366**, 155 (2010).
11. N. Permyakova, T. Zheltonozhskaya, O. Demchenko, L. Momot, S. Filipchenko, V. Syromyatnikov *Ukr. chem.J.* **68**, 123 (2002).
12. B. Sergeev, L. Lopatina, A. Prusov, G. Sergeev, *Colloid. J.* **67**, 79 (2005).
13. N.N. Maltceva, V.S. Hain, *Sodium borohydride. Characteristic and application* (Nauka, Moscow, 1985).
14. Yu.S. Lipatov, V.V. Shilov, Yu.P. Gomza et al. *X-Ray Diffraction Methods to Study Polymeric Systems* (Nauk. Dumka, Kyiv, 1982).
15. G. Beaucage, J. Hyeonlee, S. Pratsinis, S. Vemury, *Langmuir* **14**, 5751 (1998).
16. G. Schmid, *In Nanoparticles: From theory to application.* (Weinheim: Wiley–CH Verlag GmbH & Co, 2004).
17. A. Henglein *J. Phys. Chem.* **97**, 5457 (1993).
18. E.A. Becturov, S.E. Kudaybergenov, A.K. Garmagambetova, R.M. Iskakov, J.E. Ibraeva, S.N. Shmakov *Polymer-protected metal nanoparticles* (Almaty, 2010).
19. A.P Shpak., V.V. Shilov, O.A. Shilova, Yu.A. Kunitskiy *Diagnostics of nanosystems. Multilevel fractal structures* (Nauk. Dumka, Kyiv, 2004).